Palestine Journal of Mathematics

Vol 14(3)(2025) , 1102–1119

MATHEMATICAL ANALYSIS OF TWO VARIANTS OF COVID-19 MODEL THROUGH FRACTIONAL AND INTEGER ORDER

Zia Ullah, Muhammad Shoaib Arif, Rahim Ud Din and Ikram Ullah

Communicated by Thabet Abdeljawad

MSC 2020 Classifications: Primary 20M99, 13F10; Secondary 13A15, 13M05.

Keywords and phrases: $SEI_cI_DI_MR$ model; Omicron; Delta; Covid-19; Endemic equilibria; Reproduction number; Stability analysis; Grunwald-Letnikov.

The authors would like to thank the reviewers and editor for their constructive comments and valuable suggestions that improved the quality of our paper.

The authors wish to express their gratitude to Prince Sultan University for facilitating the publication of this article through the Theoretical and Applied Sciences Lab..

Corresponding Author: Rahim ud din

Abstract This study presents a mathematical analysis of the spread of two major COVID-19 variants: Delta and Omicron. The population of infected individuals is divided into three compartments, Delta-infected, Omicron-infected, and generally COVID-19-infected. First, a compartmental model is formulated using differential equations. Then, we investigate the existence, uniqueness, and basic qualitative properties of the model. The basic reproduction number $\mathcal{R}_0$ is derived using the next-generation matrix method. It is shown that if $\mathcal{R}_0 \leq 1$, the disease-free equilibrium is locally asymptotically stable. Local stability is examined via the Jacobian matrix, while global stability is analyzed using a Lyapunov function. For numerical simulations, both classical and fractional approaches are employed. The fractional model is solved using the Grunwald-Letnikov method, and the classical model is addressed using a Nonstandard Finite Difference (NSFD) scheme.

1 Introduction

Modeling for infectious diseases is a very hot topic of research in recent decades. Modeling for epidemics was introduced by McKendrick and Kermack [1]. Following that, a new compartment named Exposed (E) was established for a group of people who are not contagious and have not yet shown any symptoms. An SEIR model has been utilized to represent a variety of infectious diseases using this compartment [2]. Vaccination models [3, 4], models that take into account isolated individuals [5, 6], and even extremely detailed SIDDARTHE models [7, 8], where S stands for susceptibility, I for infected population, D for discovered, A for poor health, R for recovered, T for under treatment, H for hospitalized, and E for exposed population, have also been developed. These models are also tailored to specific disease scenarios.
In 2019, a case report in Wuhan, China, was identified as the coronavirus. On March 11, 2020, the World Health Organization (WHO) announced the new coronavirus (COVID-19) outbreak to be a global pandemic [9]. Khajanchi et al. modified the SEIR model for COVID-19 to take hospitalization plans and contact tracing into consideration while addressing COVID-19 transmission [10]. By the end of September 2020, they used model simulations to show that COVID-19 cases in India followed a power law maintained based on data from five states in the country. Samui et al. used their COVID-19 model to forecast the trajectory of infections and demonstrated the efficacy of illness rate of transmission mitigation on the fundamental reproduction number [11]. The primary goal of earlier research on epidemics [12, 13, 14] was to estimate the number of infected people based on the tactics and conditions of transmission unique to each nation.

SARS-CoV-2 transforms over time, and some of these modifications can result in new types. In order to prioritize global surveillance, study, and eventually inform the ongoing response to the COVID-19 pandemic, certain variants of concern (VOCs) had to be identified in late 2020 due to the introduction of variants that posed an enhanced risk to public health worldwide. There are five SARS-CoV-2 variants that the WHO designated as VOCs by May 31, 2021. On March 15, 2023, the WHO updated its tracking system and working definitions of VOCs, VOIs (Variant of Interest), and VUM (Variant Under Monitoring) [15]. The Omicron variant first appeared in South Africa on November 24, 2021, and it carried numerous unique genetic changes, particularly in the protein spike.
Several researchers have lately developed several kinds of models for COVID-19 using different fractional calculus techniques. In this context, very useful models have been constructed. [16].Therefore, fractional order models are more comprehensive for studying global dynamics problems in the real world. It is getting harder and harder to find exact analytical solutions for fractional-order systems. As a result, different numerical approaches have been devised in the literature for the best approximate solutions. The relevant strategies have received excellent evaluations for classical models. However, the aforementioned techniques have also been applied extensively in the situation of fractional differential equations. The non-standard finite difference (NSFD) scheme, the Euler method, and the Adam Bashforth approach are some of these schemes. Among the approaches discussed, the NSFD method is one of the most effective for estimating fractional order model solutions; see [17], [15], [16], [17], and [18] for more information.Usually, some kind of numerical procedure is employed to build a numerical system. A nonstandard finite difference scheme has been employed in this instance. This has been accomplished by applying the difference technique in this instance, which calls for the derivative to be discredited first. Furthermore, we note that a fractional differential equation's solution rarely exists in terms of a finite set of primitive functions. Therefore, in order to evaluate approximation solutions using difference schemes or other alternative methods in a realistic manner, numerical methods must be devised [18, 19, 20, 21, 22, 23, 24, 25].

2 Model Formulation

2.1 Hypotheses

To formulate COVID-19 the following assumptions are necessary.

- Human-to-human transmission occurs when symptomatic and asymptomatic infected persons come into direct or indirect contact with one another.

- There are six compartments in the infection development model at each time t. Thus, six compartments with different densities are $\mathcal{S}$, $\mathcal{E}$, $\mathcal{I}_D$, $\mathcal{I}_C$, $\mathcal{I}_M$ and $\mathcal{R}$ equal to the total population of density $\mathcal{M}(t)$.

$$\mathcal{M}(t) = \mathcal{S} + \mathcal{E} + \mathcal{I}_D + \mathcal{I}_C + \mathcal{I}_M + \mathcal{R}$$

- Deaths are not a part of the chain that spreads disease: Provided that deaths caused by COVID-19 are appropriately handled up to burial, then it is reasonable to assume that they are no longer a part of the chain that spreads the epidemic.

- Here does not exist immunity [1, 4]: those who have recovered revert to the vulnerable group following a brief period of immunity.

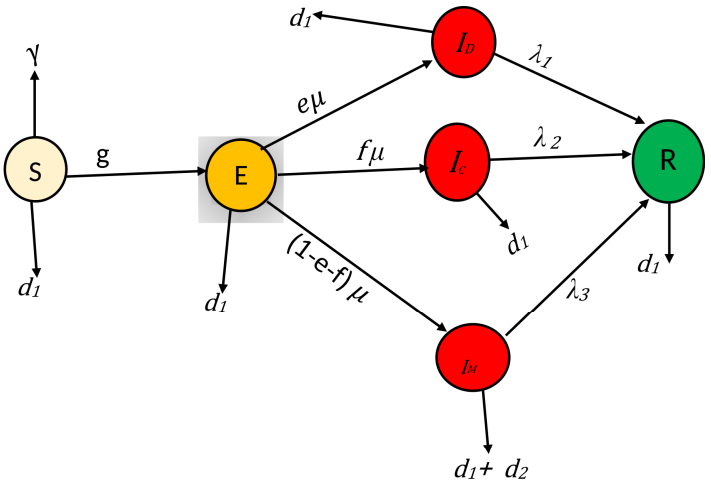

Figure 1. Diagrammatical presentation (2.1).

Based on the aforementioned assumptions, the following equations are used to explain the dynamics of COVID-19 propagation with different variants:

$$\begin{aligned}
\frac{d\mathcal{S}}{dt} &= \gamma - g\mathcal{S}\mathcal{I} - d_1\mathcal{S},\\
\frac{d\mathcal{E}}{dt} &= g\mathcal{S}\mathcal{I} - (\mu + d_1)\mathcal{E},\\
\frac{d\mathcal{I}_\mathcal{D}}{dt} &= e\mu\mathcal{E} - (\lambda_1 + d_1)\mathcal{I}_\mathcal{D},\\
\frac{d\mathcal{I}_\mathcal{C}}{dt} &= (1-e-f)\mu\mathcal{E} - (\lambda_2 + d_1 + d_2)\mathcal{I}_\mathcal{C},\\
\frac{d\mathcal{I}_\mathcal{M}}{dt} &= f\mu\mathcal{E} - (\lambda_3 + d_1)\mathcal{I}_\mathcal{M},\\
\frac{d\mathcal{R}}{dt} &= \lambda_1\mathcal{I}_\mathcal{D} + \lambda_2\mathcal{I}_\mathcal{C} + \lambda_3\mathcal{I}_\mathcal{M} - d_1\mathcal{R}.
\end{aligned} \tag{2.1}$$

Where $\mathcal{I} = \mathcal{I}_D + \mathcal{I}_C + \mathcal{I}_M$. The above equations are draw through a flow chart given below 1. Parameters, which show the transmission rate of different phenomena in above system are present in the following Table (1).

3 Boundaries, Positivity, and Feasible Region

We, get the following equation from adding all equations of model (2.1),

$$\mathcal{M}(t) = \mathcal{S}(t) + \mathcal{E}(t) + \mathcal{I}_\mathcal{D}(t) + \mathcal{I}_\mathcal{C}(t) + \mathcal{I}_\mathcal{M}(t) + \mathcal{R}(t),$$

after one has

$$\begin{aligned}
\frac{d\mathcal{M}(t)}{dt} &= \gamma - d_1\mathcal{M} - d_2\mathcal{I}_\mathcal{C}.\\
&\leq \gamma - d_1\mathcal{M},
\end{aligned} \tag{3.1}$$

from (3.1), We've got

$$\mathcal{M}(t) = \frac{\gamma}{d_1} + \left(\mathcal{M}_0 - \frac{\gamma}{d_1}\right) e^{d_1 t}. \tag{3.2}$$

Whenever t belong to the set of positive integers.

Parameters	A physical meaning in model
$\mathcal{S}$	Susceptible individuals
$\mathcal{E}$	Exposed individuals
$\mathcal{I}_{\mathcal{D}}$	Delta infected individuals
$\mathcal{I}_{\mathcal{C}}$	Covid-infected individuals
$\mathcal{I}_{\mathcal{M}}$	Omicron's infected individuals
$\mathcal{R}$	Recovered individuals
γ	New population emergence
d_1	Natural death rate
λ_1	Recovered from Delta infected
λ_2	Recovered from Covid-infected
λ_3	Recovered from an infection with Omicron
d_2	The death rate resulting from Covid-infected
e	Rate of infection by Delta virus
μ	Rate have been Exposed
f	Rate of infection by Covid-infected
g	Rate of contact

Table 1. Description of parameters and compartments used in the model (2.1).

As a result, every solution started with the system (2.1). It remains positive if and only if $t = 0$. Therefore, we say that the model (2.1) is mathematically well-posed.
By which, we get the following region in which solution of the system lies.

$$\Upsilon = (\mathcal{S}, \mathcal{E}, \mathcal{I}_{\mathcal{D}}, \mathcal{I}_{\mathcal{C}}, \mathcal{I}_{\mathcal{M}}, \mathcal{R}) : 0 \leq \mathcal{S} + \mathcal{E} + \mathcal{I}_{\mathcal{D}} + \mathcal{I}_{\mathcal{C}} + \mathcal{I}_{\mathcal{M}} + \mathcal{R} \leq \frac{\gamma}{d_1}.$$

Disease-free Equilibrium (DFE)
The disease free equilibrium (DFE) is represent by $\mathcal{E}_0$, which is equal to

$$\mathcal{E}_0 = (\mathcal{S}^0, 0, 0, 0, 0, 0).$$

That is to follow

$$\mathcal{E}^0 = \left(\frac{\gamma}{d_1}, 0, 0, 0, 0, 0\right). \tag{3.3}$$

Endemic equilibrium (EE)
Here, the endemic equilibrium (EE) is represent by E^*, which is calculated as

$$\begin{aligned}
\mathcal{S}^*(t) &= \frac{\gamma}{g\mathcal{I}^* + d_1}, \\
\mathcal{E}^*(t) &= \frac{g\gamma\mathcal{I}^*}{(g\mathcal{I}^* + d_1)(\mu + d_1)}, \\
\mathcal{I}^*_{\mathcal{D}}(t) &= \frac{ge\mu\gamma\mathcal{I}^*}{(g\mathcal{I}^* + d_1)(\mu + d_1)(\lambda_1 + d_1)}, \\
\mathcal{I}^*_{\mathcal{C}}(t) &= \frac{(1 - e - f)g\gamma\mathcal{I}^*}{(g\mathcal{I}^* + d_1)(\mu + d_1)(\lambda_1 + d_1)(\lambda_2 + d_1 + d_2)}, \\
\mathcal{I}^*_{\mathcal{M}}(t) &= \frac{gf\mu\gamma\mathcal{I}^*}{(g\mathcal{I}^* + d_1)(\mu + d_1)(\lambda_1 + d_1)(\lambda_3 + d_1)}, \\
\mathcal{R}^*(t) &= \frac{\lambda_1\mathcal{I}^*_{\mathcal{D}} + \lambda_2\mathcal{I}^*_{\mathcal{C}}\lambda_3\mathcal{I}^*_{\mathcal{M}}}{d_1}.
\end{aligned}$$

4 Expression for $\mathcal{R}_0$

The concept of the next generation matrix is used for the calculation of the basic reproduction number. From the basic reproduction number, we determine how the disease is spread through the population. When the basic reproduction number is less than or equal to 1, we say that the disease can be controlled. Let $\Upsilon = (\mathcal{E}, \mathcal{I}_{\mathcal{D}}, \mathcal{I}_{\mathcal{C}}, \mathcal{I}_{\mathcal{M}})$, after that, form the system (2.1), We've got

$$\frac{d\mathcal{Y}}{dt} = \mathcal{H} - \mathcal{U}.$$

Where

$$\mathcal{H} = \begin{pmatrix} f(g\mathcal{S}\mathcal{I}) \\ 0 \\ 0 \\ 0 \end{pmatrix},$$

and

$$\mathcal{U} = \begin{pmatrix} -(\mu + d_1)\mathcal{E} \\ -e\mu\mathcal{E} + (\lambda_1 + d_1)\mathcal{I}_{\mathcal{D}} \\ -(1 - e - f)\mu\mathcal{E} - (\lambda_2 + d_1 + d_2)\mathcal{I}_{\mathcal{C}} \\ f\mu\mathcal{E} - (\lambda_3 + d_1)\mathcal{I}_{\mathcal{M}} \end{pmatrix}.$$

The Jacobian $\mathcal{H}$ at the DFE point

$$H = \begin{pmatrix} 0 & g\mathcal{S}^0 & g\mathcal{S}^0 & g\mathcal{S}^0 \\ 0 & 0 & 0 & 0 \\ 0 & 0 & 0 & 0 \\ 0 & 0 & 0 & 0 \end{pmatrix}.$$

Moreover, for the DFE, Jacobian for the given matrix $\mathcal{U}$,

$$U = \begin{pmatrix} \mu + d_1 & 0 & 0 & 0 \\ -e\mu & \lambda_1 + d_1 & 0 & 0 \\ -(1 - e - f)\mu & 0 & \lambda_2 + d_1 + d_2 & 0 \\ -f\mu & 0 & 0 & \lambda_3 d_1 \end{pmatrix}.$$

Thus, $\mathcal{R}_0$ the spectral radius of HU^{-1} calculated as

$$\mathcal{R}_0 = \frac{gf\mu}{(\lambda_3 + d_1)(\mu + d_1)} + \frac{ge\mu}{(\lambda_1 + d_1)(\mu + d_1)} + \frac{g(1 - e - f)\mu}{(\lambda_2 + d_1 + d_2)(\mu + d_1)}.$$

Thus, $\mathcal{R}_0$ includes three parts, The first fraction shows exchanges between the infected population. Fraction in the middle shows the relation between delta infected and susceptible individuals, and the population infected with Covid-19 is shown in the last fraction part. The general population can be protected against COVID-19 infection when the valve of $\mathcal{R}_0 \leq 1$, Conversely, the infection will spread throughout the population if $\mathcal{R}_0 > 1$.
The dynamics of $\mathcal{R}_0$ in our model are present in the following figure 2, by using the numerical data from Table (2).

In next section, we briefly elaborated the stabilities of the model (2.1). Local and global stability, whenever $\mathcal{R}_0 > 1$ as well $\mathcal{R}_0 < 1$, in an equilibrium free from disease.

Theorem 4.1. *(i) For the system (2.1), there is no positive equilibrium, if* $\mathcal{R}_0 \leq 1$.
(ii)There is a clear unique positive equilibrium $\mathcal{E}^* = (\mathcal{S}^*, \mathcal{E}^*, \mathcal{I}^*_{\mathcal{D}}, \mathcal{I}^*_{\mathcal{C}}, \mathcal{I}^*_{\mathcal{M}}, \mathcal{R}^*)$*, which is also known as an endemic equilibrium develops, if* $\mathcal{R}_0 > 1$.

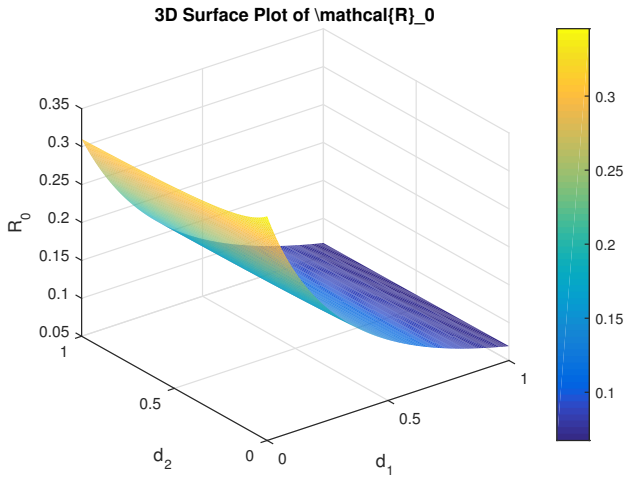

Figure 2. 3D plot of $\mathcal{R}_0$.

5 Stability Analysis

Here, in this part have local and global stability of the model (2.1). For, given endemic and disease free equilibrium points, we investigated stability of the system.

5.1 Local Stability

By using $\mathcal{R}_0 < 1$, and at disease free equilibrium $\mathcal{E}_0$ local stability for the system (2.1) is discussed in the very next theorem.

Theorem 5.1. *If $\mathcal{R}_0 < 1$, COVID-19 infection model is locally and asymptotically stable at DFE $\mathcal{E}_0$.*

Proof. The stability solution was derived by using the Jacobian Matrix as $\mathcal{E}_0$ is given here.

$$\mathcal{N} = \begin{bmatrix} -d_1 & 0 & 0 & 0 & 0 & 0 \\ 0 & -(d_1+\mu) & 0 & 0 & 0 & 0 \\ 0 & e\mu & -(\lambda_1+d_1) & 0 & 0 & 0 \\ 0 & (1-e-f)\mu & 0 & -(\lambda_2+d_1+d_2) & 0 & 0 \\ 0 & f\mu & 0 & 0 & -(\lambda_3+d_1) & 0 \\ 0 & 0 & \lambda_1 & \lambda_2 & \lambda_3 & -d_1 \end{bmatrix}$$

That Jacobian matrix's characteristic polynomial at DFE has been obtained by $det(\mathcal{N}^0 - \alpha I) = 0$, in which α represent the eigenvalue of the system, and I is stand for the identity matrix, which is 6 by 6. So, $\mathcal{N}$ the eigenvalues provided by

$$\begin{aligned} \alpha_1 &= -d_1, \\ \alpha_2 &= -(\mu + d_1), \\ \alpha_3 &= -(\lambda_1 + d_1), \\ \alpha_4 &= -(\lambda_2 + d_1 + d_2), \\ \alpha_5 &= -(\lambda_3 + d_1), \\ \alpha_6 &= -d_1. \end{aligned}$$

α_1, α_2, α_3, α_4, α_5 and α_6 are strictly negative. Thus, Local asymptotically stability corresponds to disease free stability (DEF) is achieved. □

5.2 Global Stability

Global stability of the system (2.1) is investigated through Lyapunov function. By using $\mathcal{R}_0 \leq 1$ and at disease free equilibrium state $\mathcal{E}_0$, In next theorem the global stability is presented.

Theorem 5.2. *If $\mathcal{R}_0 \leq 1$, then the system (2.1) is globally asymptotically stable at $\mathcal{E}_0$.*

Proof. To calculate global stability of model (2.1), we used Lyapnuov function concept, which is construct as

$$\mathcal{V} = K_1(\mathcal{S} - \mathcal{S}^0) + K_2(\mathcal{E} - \mathcal{E}^0) + K_3(\mathcal{I}_\mathcal{D} - \mathcal{I}_\mathcal{D}{}^0) + K_4(\mathcal{I}_\mathcal{C} - \mathcal{I}_\mathcal{C}{}^0) + K_5\mathcal{I}_\mathcal{M}. \tag{5.1}$$

This K_1, K_2, K_3 , K_4 and K_5 consist of a few constants. Now, take derivative w.r.t "t" of the equation above.

$$\dot{\mathcal{V}} = K_1\dot{\mathcal{S}} + K_2\dot{\mathcal{E}} + K_3\dot{\mathcal{I}_\mathcal{D}} + K_4\dot{\mathcal{I}_\mathcal{C}} + K_5\dot{\mathcal{I}_\mathcal{M}}.$$

Using the values from (2.1)

$$\begin{aligned}\dot{\mathcal{V}} &= K_1\gamma - f(g\dot{\mathcal{S}\mathcal{I}}) - d_1\mathcal{S} + K_2 f(g\mathcal{S}\mathcal{I}) - \dot{(\mu + d_1)}\mathcal{E} + K_3 e\mu\mathcal{E} + (\dot{\lambda_1} + d_1)\mathcal{I}_\mathcal{D} \\ &+ K_4(1 - e - f)\mu\mathcal{E} + \dot{(\lambda_2 + d_1 + d_2)}\mathcal{I}_\mathcal{C} + K_5 f\mu\mathcal{E} + (\lambda_3 + d_1)\mathcal{I}_\mathcal{M}.\end{aligned}$$

With some basic calculations

$$\begin{aligned}\dot{V} &= f(g\mathcal{S}\mathcal{I})(K_2 - K_1) + e\mu\mathcal{E}(K_3 - K_4) + \mu\mathcal{E}(K_4 - K_2) + f\mu\mathcal{E}(K_5 - K_4) \\ &- (K_1 d_1\mathcal{S} - K_1\gamma) - K_2 d_1\mathcal{E} - K_3\lambda_1\mathcal{I}_\mathcal{D} - K_3 d_1\mathcal{I}_\mathcal{D} - K_4\lambda_2\mathcal{I}_\mathcal{C} - K_4 d_1\mathcal{I}_\mathcal{C} - K_4 d_2\mathcal{I}_\mathcal{C} - K_5\lambda_3\mathcal{I}_\mathcal{M} - K_5 d_1\mathcal{I}_\mathcal{M}.\end{aligned}$$

assumed that $K_1 = K_2 = K_3 = K_4 = K_5 = 1$.
which implies

$$\dot{V} = -(d_1\mathcal{S} - \gamma) - d_1\mathcal{E} - \lambda_1\mathcal{I}_\mathcal{D} - d_1\mathcal{I}_\mathcal{D} - \lambda_2\mathcal{I}_\mathcal{C} - d_2\mathcal{I}_\mathcal{C} - \lambda_3\mathcal{I}_\mathcal{M} - d_1\mathcal{I}_\mathcal{M} < 0$$

Which show that the model (2.1) is asymptotically globally stable, whenever $\mathcal{R}_0 \leq 1$, which follow conclusion. □

6 A Discussion and Numerical Results

We consider the cases of infection that have been reported globally. Daily assessments of the infection are conducted with the use of a unit per day. Let suppose developed the natural birth and death rates for our model 0.0155432, to determine the average death age in 2020 − 21, through the defined model (2.1), just two out of the 12 parameters. The procedures $M(0) = \frac{\gamma}{d_1}$. Whenever figuring out the birth rates, That $M(0)$ represents the total population. Let supposed $M(0) = 60140000$ population is estimated for our model. $\mathcal{S}(0) = 60069540$ when the disease does not appear in an individual member of the uninfected group of people, and $\mathcal{E}(0) = 0.062million, \mathcal{I}_\mathcal{D}(0) = 0.008million, \mathcal{I}_\mathcal{C}(0) = 100$, and $\mathcal{I}_\mathcal{M}(0) = 360$ is the people listed here, with $\mathcal{R}(0) = 0$ having the original set of parameters susceptible to fit the data in. Assume that there has been no progress in recovery from the infection. The Non standard finite difference scheme (NSFD) method is applied to adapt the system to the provided numerical data at the time frame mentioned earlier. The experiments were conducted until the model fitting accuracy reached the necessary level. At this point the NSFD system is constructed [32] over the model we are considering. So have a look at the first equation of (2.1) when

$$\frac{d\mathcal{S}(t)}{dt} = \gamma - f(g\mathcal{S}\mathcal{I}) - d_1\mathcal{S}. \tag{6.1}$$

Here the NSFD mechanism enters in

$$\frac{\mathcal{S}_{i+1} - \mathcal{S}_i}{h} = \gamma - g\mathcal{S}_i\mathcal{A}_i - d_1\mathcal{S}_i. \tag{6.2}$$

Nomenclature	Numerical values
$\mathcal{S}$	6.0069540 x 10^6
$\mathcal{E}$	0.062000 x 10^6
$\mathcal{I}_{\mathcal{D}}$	0.008000 x 10^6
$\mathcal{I}_{\mathcal{C}}$	0.000100 x 10^6
$\mathcal{I}_{\mathcal{M}}$	0.000360 x 10^6
$\mathcal{R}$	0 x 10^6
γ	0.2553
d_1	0.00425
λ_1	0.8447
λ_2	0.200
λ_3	0.6746
d_2	0.0015
f	0.0101
μ	0.8999
e	0.9566
g	0.8999

Table 2. Numerical values of parameters and compartments used in the model (2.1).

such a way (6.2), Then use the NSFD approach to present the model. (2.1) whenever

$$\begin{aligned}
\mathcal{S}_{i+1} &= \mathcal{S}_i + h\Big(\gamma - g\mathcal{S}_i\mathcal{S}_i - d_1\mathcal{S}_i\Big),\\
\mathcal{E}_{i+1} &= \mathcal{E}_i + h\Big(g\mathcal{S}_i\mathcal{A}_i - (\mu + d_1)\mathcal{E}_i\Big), \qquad (6.3)\\
\mathcal{I}_{\mathcal{D}i+1} &= \mathcal{A}_i + h\Big(e\mu\mathcal{E}_i - (\lambda_1 + d_1)\mathcal{I}_{\mathcal{D}i}\Big) \qquad (6.4)\\
\mathcal{I}_{\mathcal{C}i+1} &= \mathcal{U}_i + h\Big((1 - e - f)\mu\mathcal{E}_i - (\lambda_2 + d_1 + d_2)\mathcal{I}_{\mathcal{C}i}\Big), \qquad (6.5)\\
\mathcal{I}_{\mathcal{M}i+1} &= \mathcal{R}_i + h\Big(f\mu\mathcal{E}_i - (\lambda_3 + d_1)\mathcal{I}_{\mathcal{M}i}\Big),\\
\mathcal{R}_{i+1} &= \mathcal{R}_i + h\Big(\lambda_1\mathcal{I}_{\mathcal{D}i} + \lambda_2\mathcal{I}_{\mathcal{C}i} + \lambda_3\mathcal{I}_{\mathcal{M}i} - d_1\mathcal{R}_i\Big).
\end{aligned}$$

Designing the NSFD scheme [32], We represented the model with a plot (2.1). Understanding the system's dynamics demands, For simulation, we used global general data. First, we use real data from [33], to estimate the transmission rates for each strain using Non standard finite difference scheme NSFD. Using Table(2), we determine their graphical analysis for every strain based on the obtained transmission rate. The above figures (3-8) highlight the dynamical behavior of the system (2.1). We suggest that, preventive actions like social distance, immunization, and COVID-19 patient testing and treatment are included in the three strategies to over come this disease. Since there are two strains in our model, delta and Omicron, we can examine the effectiveness of each method for each strain independently. We used MATLAB to carry out the simulation.

7 Scheme of NSFD for Fractional Order Model (2.1)

We provide some fractional concepts for model (2.1), in this part of our paper . We applied the Grunwald-Letnikov approach, that has been used the authors in [34, 35]. We used this method to

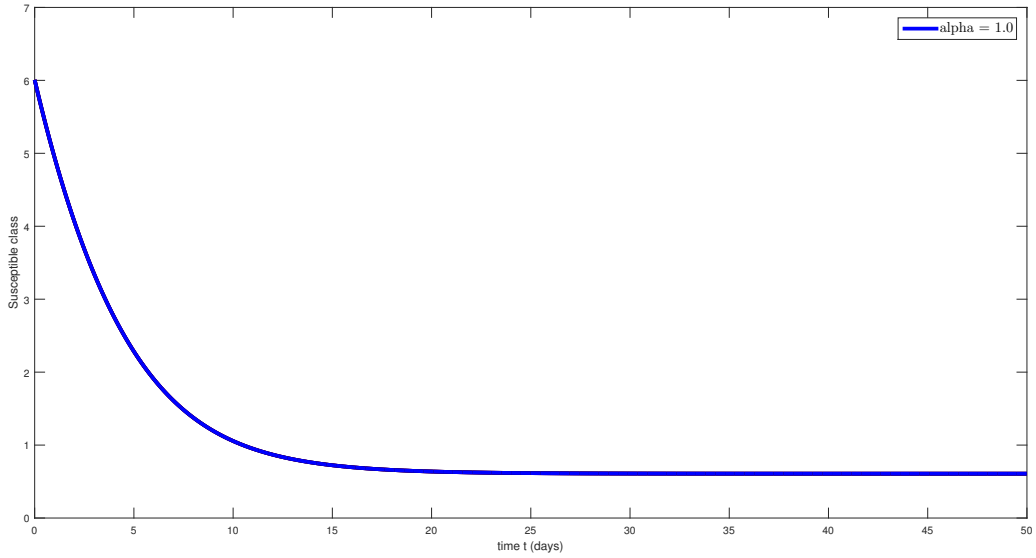

Figure 3. NSFD numerical scheme plot for corresponding dynamic behaviors of the model of susceptible compartment.

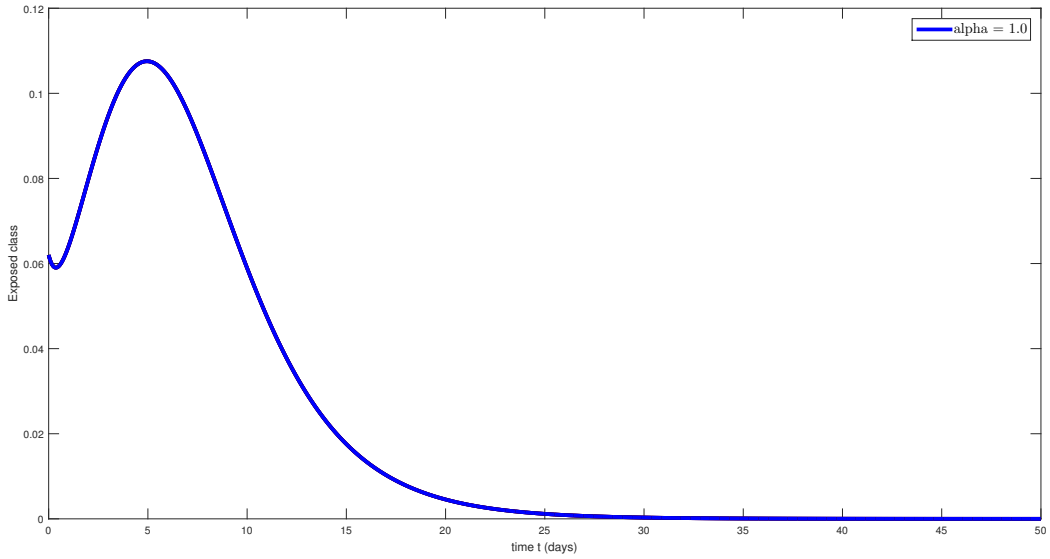

Figure 4. NSFD numerical scheme plot for corresponding dynamic behaviors of the model of exposed compartment.

present the dynamical behavior of the system (2.1). To investigate stabilities of the system (2.1) under disease free and endemic equilibrium point and small interval of h support this fractional method. The Euler, RK2, and RK4 methods were the most commonly utilized techniques by researchers; however, this numerical method has advantages over them. compared to the RK2 and RK4 methods, this specific numerical scheme is less difficult and more accurate. This numerical method gives effective numerical results over a long period of time, which gives it an impressive advantage over different methods.

Definition 7.1. "Non-integer order integral $\gamma > 0$ having a particular function $\mathcal{S} : [0, \infty) \to \mathbb{R}$ is

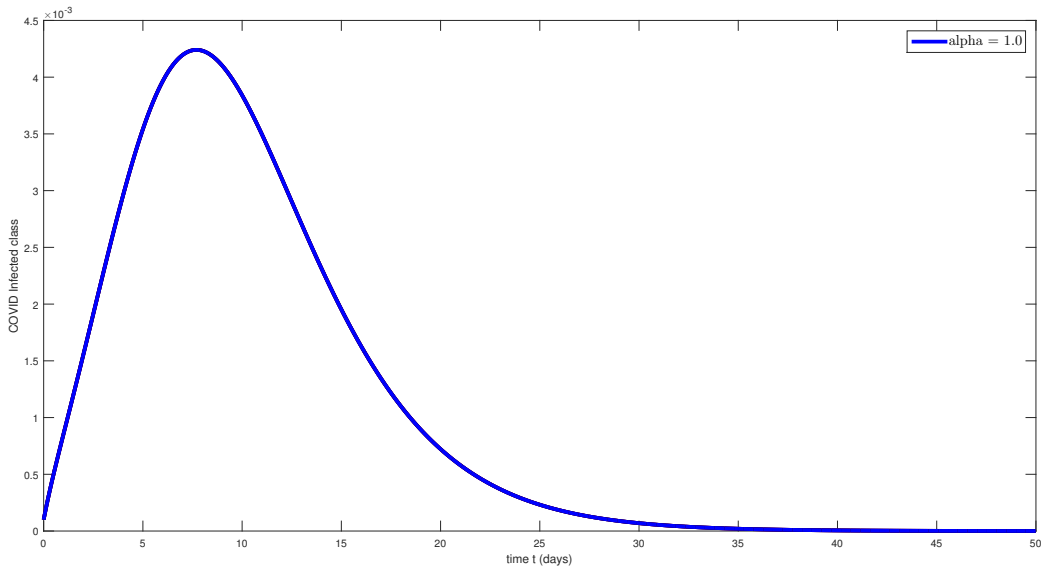

Figure 5. NSFD numerical scheme plot for corresponding dynamic behaviors of the model of COVID infected compartment.

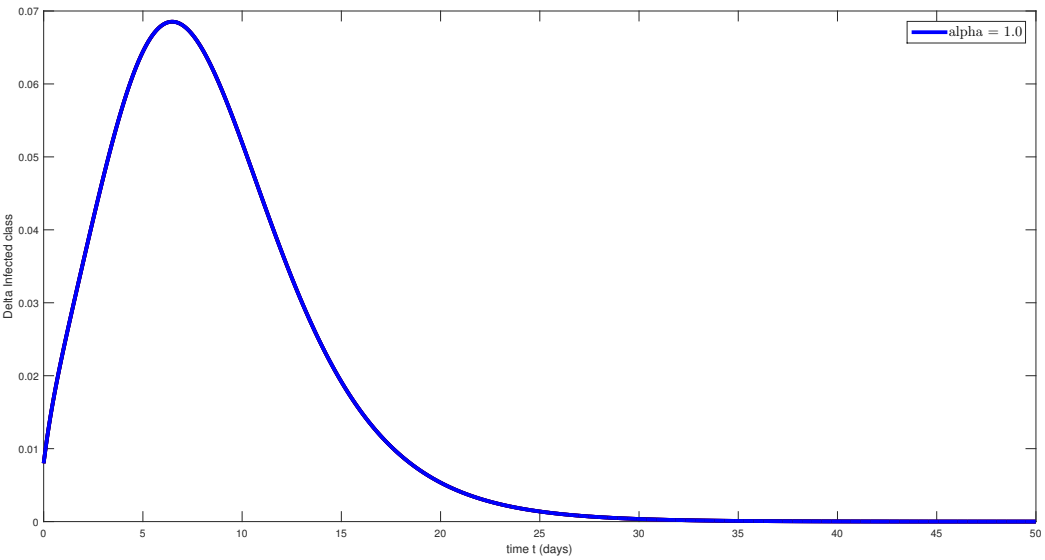

Figure 6. NSFD numerical scheme plot for corresponding dynamic behaviors of the model of delta virus infected compartment.

described as

$$A_t^{\sigma}\mathcal{Y}(t) = \frac{1}{\Upsilon(\beta)}\int_0^t \frac{\mathcal{Y}(\theta)}{(t-\theta)^{1-\beta}}d\theta,$$

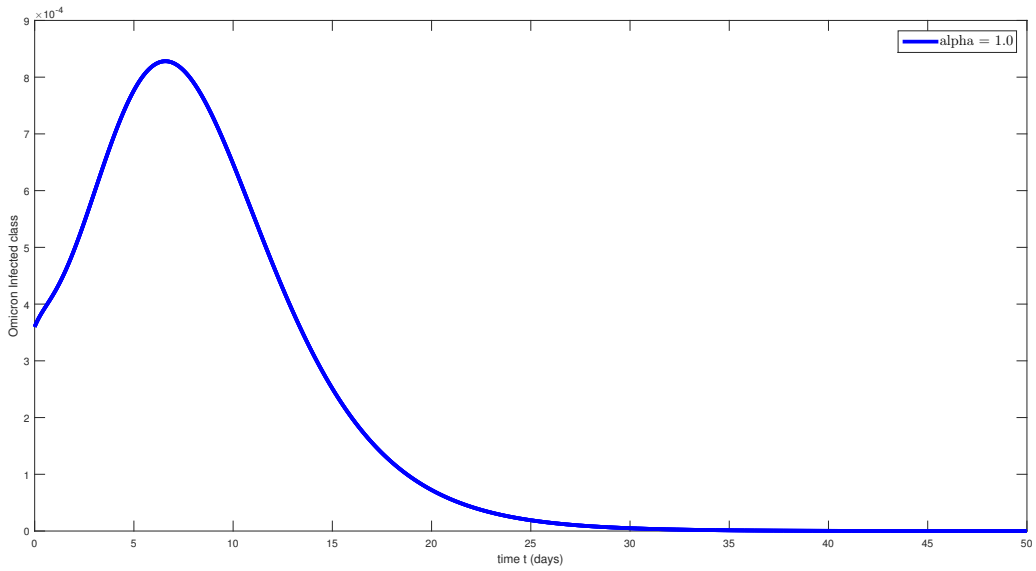

Figure 7. NSFD numerical scheme plot for corresponding dynamic behaviors of the model of omicron virus infected compartment.

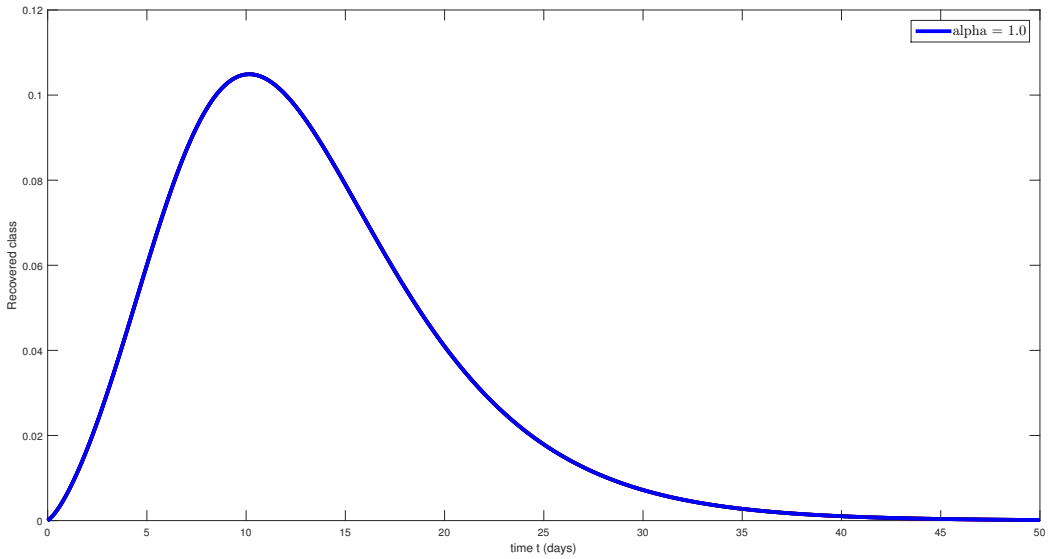

Figure 8. NSFD numerical scheme plot for corresponding dynamic behaviors of the model of recovered compartment.

assume the integral is present at the right sides." Moreover, by definition of Caputo, we have

$$D_{0+}^{\beta}\mathcal{Y}(t) = \begin{cases} \dfrac{1}{\Upsilon(1-\beta)}\displaystyle\int_0^t (t-\mu)^{-\beta}\mathcal{Y}'(\mu)d\mu, \ 0 < \beta \leq 1, \\ \dfrac{d\mathcal{Y}}{dt}, \ \ \beta = 1. \end{cases}$$

From Riemann Liouville integral operator of a certain fractional order as

$$A^{\beta}\Upsilon(t) = \frac{1}{\Gamma(\beta)}\int_0^t (t-\tau)^{\beta-1}\Upsilon(\theta)d\theta,\ \beta > 0. \tag{7.1}$$

After the process which used the author in [36],We've got

$${}^{k}\mathrm{D}^{\beta}\Upsilon(t) = \sum_{i=0}^{m+1} M_i^{\beta}\Upsilon_{n-i+1},\ m = 0,1,2,..., \tag{7.2}$$

in which $M_0 = \frac{1}{\mathfrak{h}^{\beta}}$, $M_i = \left(\frac{i-1-\beta}{i}\right)M_{i-1}^{\beta}$, $i = 1,2,3,....$ It's interesting in this case when $m = 0$,
From, we have (7.2)

$${}^{k}\mathrm{D}^{\beta}\Upsilon(t) = \frac{\Upsilon_1 - \beta\Upsilon_0}{\mathfrak{h}^{\beta}}.$$

Consider

$$\begin{cases} {}^{k}\mathrm{D}^{\beta}\Upsilon(t) = f(t,\Upsilon(t)),\ t \in [0,T], 0 < T < \infty, \\ \Upsilon(t_0) = \Upsilon_0. \end{cases} \tag{7.3}$$

Using equation (7.2) to discretion (7.3) as

$$\sum_{i=0}^{m+1} M_i^{\alpha}\Upsilon_{m-i+1} = f(t_{m+1},\Upsilon(t_{m+1})),\ m = 0,1,2,..., \tag{7.4}$$

We've got

$$\Upsilon_{m+1} = \frac{1}{M_0^{\beta}}\left[-\sum_{i=1}^{m+1} M_i^{\beta}\Upsilon_{m-i+1} + f(t_{m+1},\Upsilon(t_{m+1}))\right],\ \text{where } m = 0,1,2,..., \tag{7.5}$$

in which $M_0^{\beta} = \left[\frac{1}{\sigma(\mathfrak{h},\omega)}\right]^{\beta}$, $M_i^{\beta} = \left[\frac{i-1-\beta}{i}\right]M_{i-1}^{\beta}$, $i = 1,2,3,....$ Let's say $\sigma(\mathfrak{h},\omega)$ obtained $\mathfrak{h} + O(\mathfrak{h}^2)$. Several functions provide the stability rule, such as $\sin\mathfrak{h}, \cos\mathfrak{h}, \mathfrak{h}$, etc. We now present our counseling system (2.1) as instead of non-integral order $0 < \beta \leq 1$ as follows

$$\begin{cases} {}^{k}\mathrm{D}^{\beta}S(t) = \gamma - (g\mathcal{S}\mathcal{I}) - d_1\mathcal{S}, \\ {}^{k}\mathrm{D}^{\beta}E(t) = (g\mathcal{S}\mathcal{I}) - (\mu + d_1)\mathcal{E}, \\ {}^{k}\mathrm{D}^{\beta}I_D(t) = e\mu\mathcal{E} - (\lambda_1 + d_1)\mathcal{I}_{\mathcal{D}}, \\ {}^{k}\mathrm{D}^{\beta}I_C(t) = (1-e-f)\mu\mathcal{E} - (\lambda_2 + d_1 + d_2)\mathcal{I}_{\mathcal{C}}, \\ {}^{k}\mathrm{D}^{\beta}I_M(t) = f\mu\mathcal{E} - (\lambda_3 + d_1)\mathcal{I}_{\mathcal{M}}, \\ {}^{k}\mathrm{D}^{\beta}R(t) = \lambda_1\mathcal{I}_{\mathcal{D}} + \lambda_2\mathcal{I}_{\mathcal{C}} + \lambda_3\mathcal{I}_{\mathcal{M}} - d_1\mathcal{R}. \end{cases} \tag{7.6}$$

Considering of (7.5) and by the use of the Grunwald-Letnikov discrimination method, for system

(7.6), We introduce a numerical method here for non-integral order.

$$
\begin{cases}
S(t_{m+1}) = \dfrac{1}{M_0^{\beta}}\Big[-\displaystyle\sum_{i=1}^{m+1} M_i^{\beta} S(t_{m+1-i}) + \gamma - g\mathcal{S}(t_m)\mathcal{A}(t_m) - d_1\mathcal{S}(t_m)\Big], \\
E(t_{m+1}) = \dfrac{1}{M_0^{\beta}}\Big[-\displaystyle\sum_{i=1}^{m+1} M_i^{\beta} E(t_{m+1-i}) + g\mathcal{S}(t_m)\mathcal{A}(t_m) - (\mu + d_1)\mathcal{E}(t_m)\Big], \\
I_D(t_{m+1}) = \dfrac{1}{M_0^{\beta}}\Big[-\displaystyle\sum_{i=1}^{m+1} M_i^{\beta} I_D(t_{m+1-i}) + e\mu\mathcal{E}(t_m) + (\lambda_1 + d_1)\mathcal{I}_{\mathcal{D}}(t_m)\Big], \\
I_C(t_{m+1}) = \dfrac{1}{M_0^{\beta}}\Big[-\displaystyle\sum_{i=1}^{m+1} M_i^{\beta} I_C(t_{m+1-i}) + (1-e-f)\mu\mathcal{E}(t_m) + (\lambda_2 + d_1 + d_2)\mathcal{I}_{\mathcal{C}}(t_m)\Big], \\
I_M(t_{m+1}) = \dfrac{1}{M_0^{\beta}}\Big[-\displaystyle\sum_{i=1}^{m+1} M_i^{\beta} I_M(t_{m+1-i}) + f\mu\mathcal{E}(t_m) + (\lambda_3 + d_1)\mathcal{I}_{\mathcal{M}}(t_m) \\
R(t_{m+1}) = \dfrac{1}{M_0^{\beta}}\Big[-\displaystyle\sum_{i=1}^{m+1} M_i^{\beta} R(t_{m+1-i}) + \lambda_1\mathcal{I}_{\mathcal{D}}(t_m) + \lambda_2\mathcal{I}_{\mathcal{C}}(t_m) + \lambda_3\mathcal{I}_{\mathcal{M}}(t_m) - d_1\mathcal{R}(t_m)\Big].
\end{cases}
\tag{7.7}
$$

Figures here (8-14), We use different fractional orders to graphically represent the dynamical behaviors of different classes.

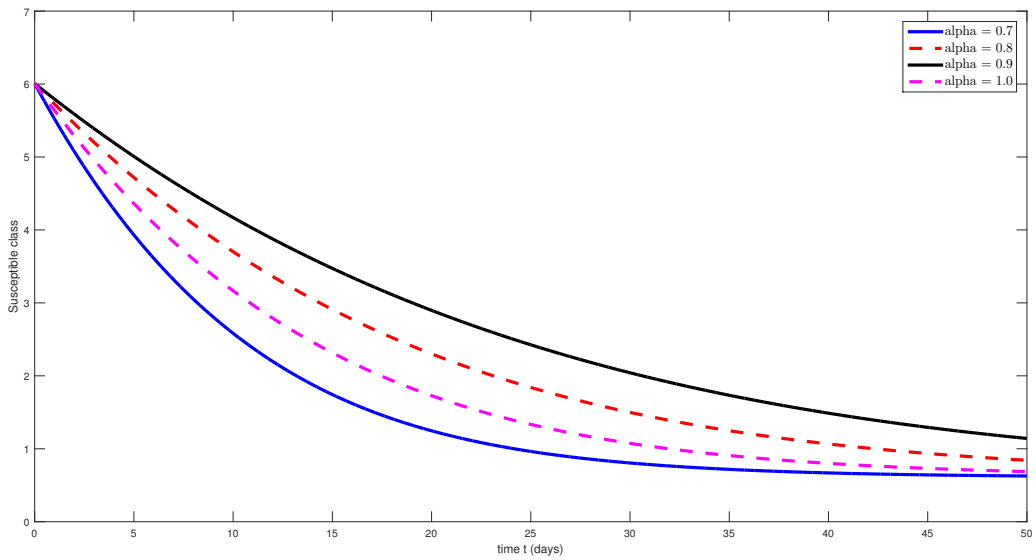

Figure 9. Fractional numerical scheme plot for corresponding dynamic behaviors of the model of susceptible compartment.

Using Grunwald-Letnikov method, we present the dynamical behavior of system (2.1). Numerical data used from from Table 2, the figures (3-8), show fractional graphical analysis of the system.

8 Conclusion

In this paper, we provide a mathematical model that takes into account several strains and simulates optimal control by choosing widely used tactics like social separation, immunisation, and testing-treatment. Three equilibrium points disease-free equilibrium, variant 1 endemic equilibrium, and variant 2 endemic equilibrium as well as the positivity and boundedness of the

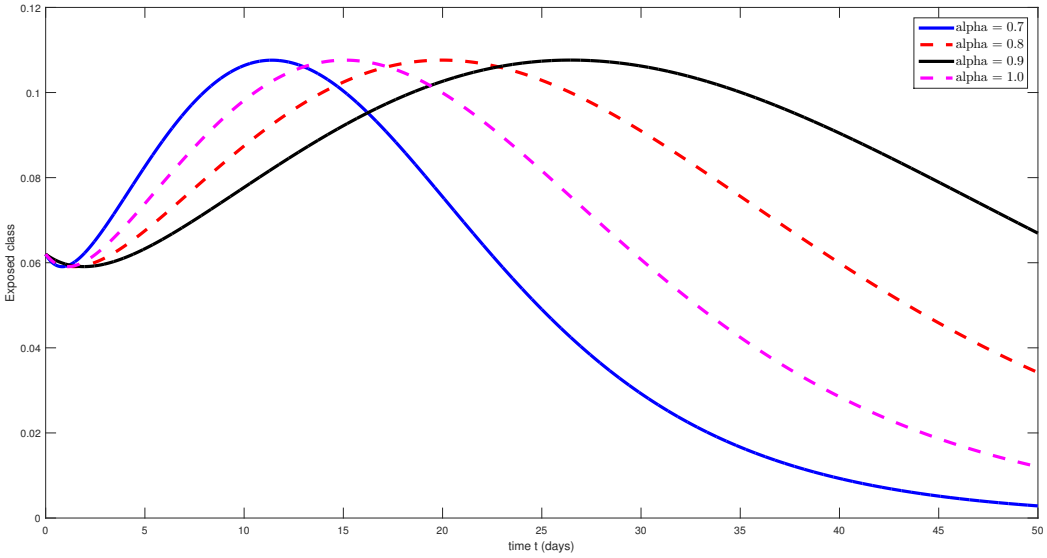

Figure 10. Fractional numerical scheme plot for corresponding dynamic behaviors of the model of exposed compartment.

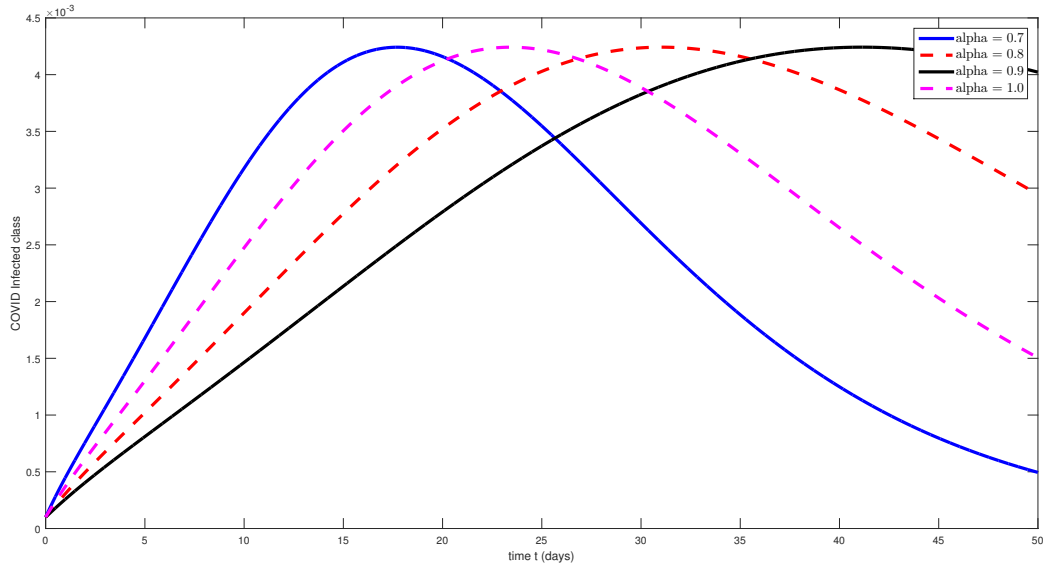

Figure 11. Fractional numerical scheme plot for corresponding dynamic behaviors of the model of COVID infected compartment.

outcome were taken into consideration when establishing the model.
In summary, at each stage, the number of infected people with the Omicron virus $(\mathcal{I}_M)$ is substantially more than that of the Delta virus $(\mathcal{I}_D)$. Furthermore, less individuals will become infected and exposed to the virus if controls are more tight. The top rises from the mild to ordinary level, suggesting that there would be ample time to get ready before it peaks. This has the effect of delaying both the peak number of afflicted people and the infectious disease's elimination. However, when the control method is applied strictly, there is a certain amount of reduction. This indicates that effective social distancing strategies advance the endemic's endpoint by significantly lowering the number of affected people, going beyond just flattening the

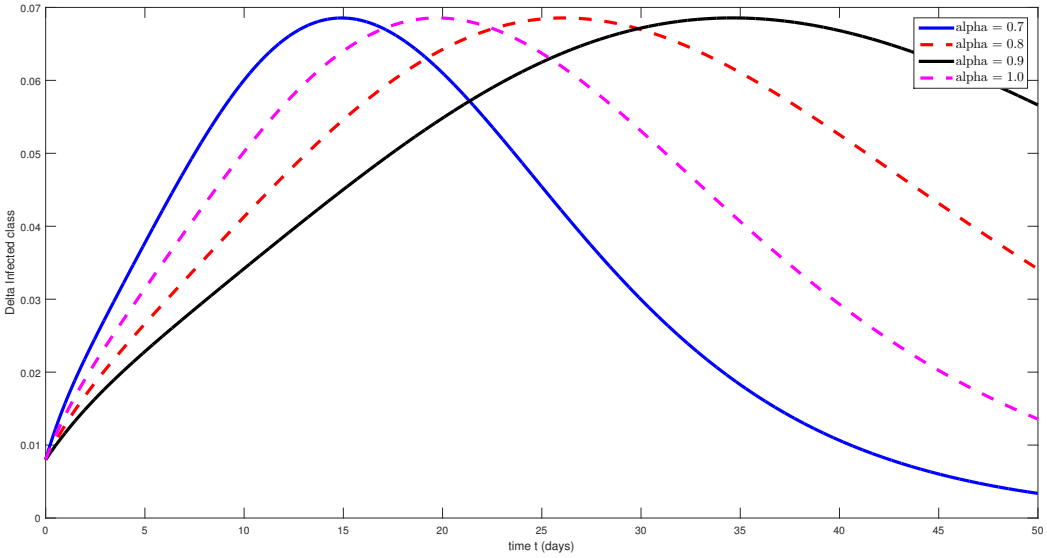

Figure 12. Fractional numerical scheme plot for corresponding dynamic behaviors of the model of delta virus compartment.

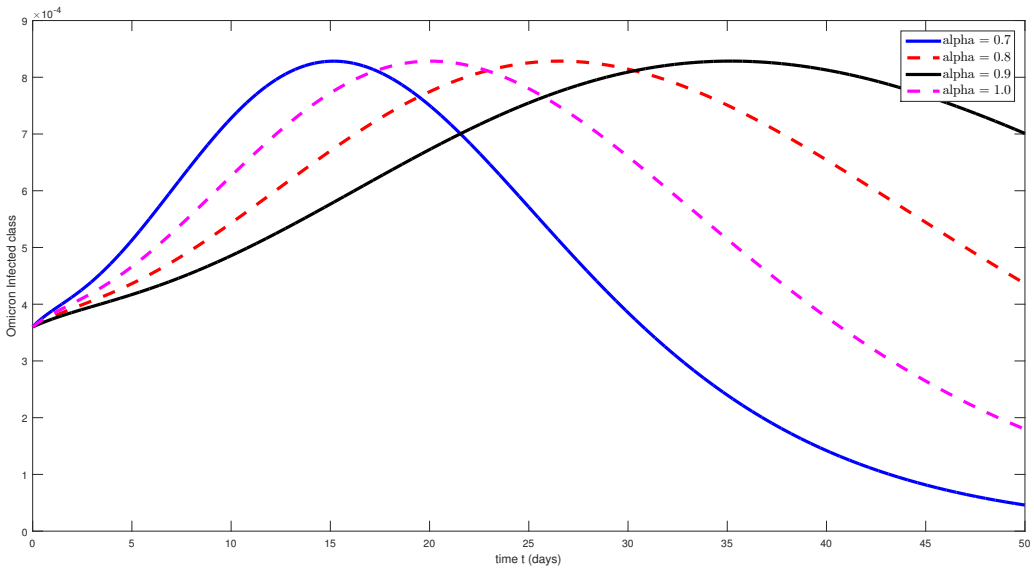

Figure 13. Fractional numerical scheme plot for corresponding dynamic behaviors of the model of omicron infected compartment.

infection curve.

References

[1] Ud Din, Rahim, Kamal Shah, Imtiaz Ahmad, and Thabet Abdeljawad. Study of transmission dynamics of novel COVID-19 by using mathematical model. *Advances in Difference Equations* 2020, (2020), 1-13.

[2] Shah, Kamal, Rahim Ud Din, Wejdan Deebani, Poom Kumam, and Zahir Shah. On nonlinear classical and fractional order dynamical system addressing COVID-19. *Results in Physics* 24, (2021), 104069.

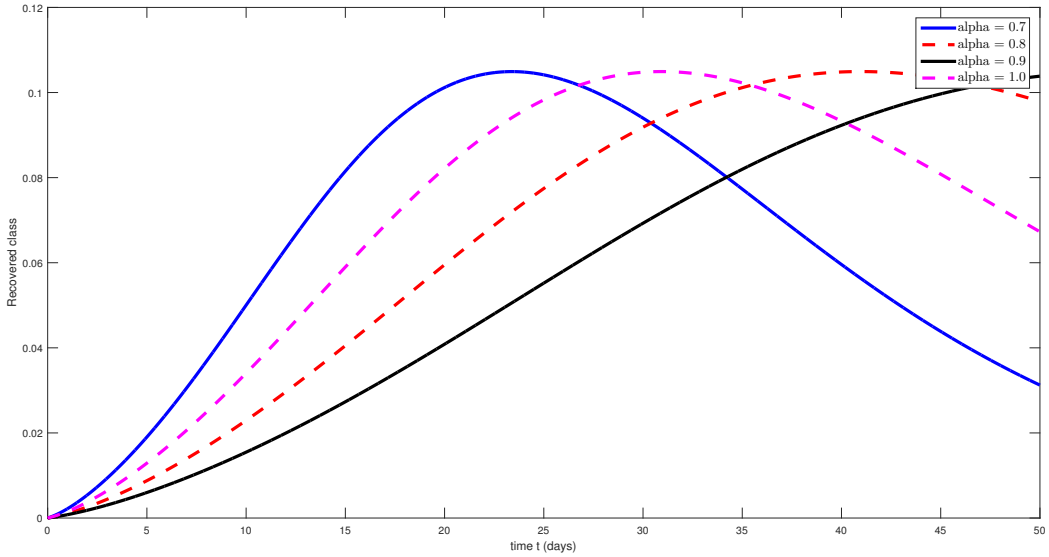

Figure 14. Fractional numerical scheme plot for corresponding dynamic behaviors of the model of recovered compartment.

[3] Shah, Kamal, and Thabet Abdeljawad. Study of a mathematical model of COVID-19 outbreak using some advanced analysis. *Waves in random and complex media* (2022): 1-18.

[4] Shah, Kamal, Muhammad Sinan, Thabet Abdeljawad, Mohammed A. El-Shorbagy, Bahaaeldin Abdalla, and Marwan S. Abualrub. A Detailed Study of a Fractal-Fractional Transmission Dynamical Model of Viral Infectious Disease with Vaccination. *Complexity* 2022(1), (2022), 7236824.

[5] Karthikeyan, Kulandhivel, Panjaiyan Karthikeyan, Haci Mehmet Baskonus, Kuppusamy Venkatachalam, and Yu-Ming Chu. Almost sectorial operators on Hilfer derivative fractional impulsive integro-differential equations. *Mathematical Methods in the Applied Sciences* 45(13), (2022), 8045-8059.

[6] Saima Rashid, Sobia Sultana, Yeliz Karaca, Aasma Khalid, Yu-Ming Chu, Some further extensions considering discrete proportional fractional operators, *Fractals* 30(01), (2022), 2240026.

[7] Rashid, Saima, Elbaz I. Abouelmagd, Sobia Sultana, and Yu-Ming Chu. "New Developments in Weighted n-Fold Type Inequalities via Discrete Generalized Proportional Fractional Operators. *Fractals* 30(02), (2022), 2240056.

[8] Zibaei, S. A. D. E. G. H., and M. I. E. H. R. A. N. Namjoo. A nonstandard finite difference scheme for solving fractional-order model of HIV-1 infection of CD4+ T-cells. (2015): 169-184.

[9] Din, Anwarud, et al. Mathematical analysis of spread and control of the novel corona virus (COVID-19) in China. *Chaos, Solitons and Fractals* 141, (2020), 110286.

[10] Sweilam, N. H., A. M. Nagy, and L. E. Elfahri. Nonstandard finite difference scheme for the fractional order Salmonella transmission model. *J. Fract. Calc. Appl* 10, (2019), 197-212.

[11] Liu, Fawang, and Kevin Burrage. Novel techniques in parameter estimation for fractional dynamical models arising from biological systems. *Computers & Mathematics with Applications* 62(3), (2011), 822-833.

[12] Algehyne, Ebrahem A., and Rahim ud Din. On global dynamics of COVID-19 by using SQIR type model under non-linear saturated incidence rate. *Alexandria Engineering Journal* 60(1), (2021), 393-399.

[13] Wang, Fuzhang, Muhammad Nawaz Khan, Imtiaz Ahmad, Hijaz Ahmad, Hanaa Abu-Zinadah, and Yu-Ming Chu. "Numerical solution of traveling waves in chemical kinetics: time-fractional fishers equations. *Fractals* 30(02), (2022), 2240051.

[14] Fathalla A. Rihan, Hebatallah J. Alsakaji, C. Rajivganthi, Stochastic SIRC epidemic model with time-delay for COVID-19, *Adv. Difference Equ.* 2020(1), (2020) 1-20.

[15] Zizhen Zhang, A novel covid-19 mathematical model with fractional derivatives: Singular and nonsingular kernels, *Chaos Solitons Fractals* 139(2020), 110060.

[16] Shah, Kamal, Thabet Abdeljawad, Ibrahim Mahariq, and Fahd Jarad. Qualitative analysis of a mathematical model in the time of COVID-19. *BioMed Research International* 2020(1), (2020), 5098598.

[17] Zhao, Shi, Qianyin Lin, Jinjun Ran, Salihu S. Musa, Guangpu Yang, Weiming Wang, Yijun Lou et al. Preliminary estimation of the basic reproduction number of novel coronavirus (2019-nCoV) in China, from 2019 to 2020: A data-driven analysis in the early phase of the outbreak. International journal of infectious diseases 92, (2020), 214-217.

[18] Dai, Zoujun, Ying Peng, Hansen A. Mansy, Richard H. Sandler, and Thomas J. Royston. A model of lung parenchyma stress relaxation using fractional viscoelasticity. *Medical engineering & physics* 37(8), (2015), 752-758.

[19] Matlob, Mohammad Amirian, and Yousef Jamali. The concepts and applications of fractional order differential calculus in modeling of viscoelastic systems: A primer. *Critical* $Reviews^{TM}$ *in Biomedical Engineering* 47(4), (2019), 249-276.

[20] Aghriche, A., Mathematical Model of COVID-19 Transmission with Education Campaign and Treatment Through Quarantine. *Palestine Journal of Mathematics*, 14(1) 2025.

[21] El Ghabi, M., H. Alaa, F. Aqel, and N. E. Alaa. Nonlinear boundary periodic equation with arbitrary growth nonlinearity and data measure: Mathematical analysis and Numerical simulation by LBM method. Palestine Journal of Mathematics 13(4), (2024).

[22] Mohammed, Azhi Sabir, and Sarbaz HA Khoshnaw. The Impact of Vaccination on COVID-19 Pandemic in the Kurdistan Region of Iraq: A Mathematical Modelling. *Palestine Journal of Mathematics*, 12, 2023.

[23] Grzesikiewicz, Wieslaw, Andrzej Wakulicz, and Artur Zbiciak. Non-linear problems of fractional calculus in modeling of mechanical systems. *International Journal of Mechanical Sciences* 70, (2013), 90-98.

[24] Celauro, C., C. Fecarotti, A. Pirrotta, and A. C. Collop. Experimental validation of a fractional model for creep/recovery testing of asphalt mixtures. *Construction and Building Materials* 36,(2012), 458-466.

[25] Lewandowski, Roman, and ZdzisLaw Pawlak. Dynamic analysis of frames with viscoelastic dampers modelled by rheological models with fractionalderivatives. *Journal of sound and Vibration* 330(5), (2011), 923-936.

[26] Shah, Kamal, Thabet Abdeljawad, Arshad Ali, and Manar A. Alqudah. Investigation of integral boundary value problem with impulsive behavior involving non-singular derivative. *Fractals* 30(08), (2022), 2240204.

[27] Hamza, Amjad E., Osman Osman, Arshad Ali, Amer Alsulami, Khaled Aldwoah, Alaa Mustafa, and Hicham Saber. Fractal-Fractional-Order Modeling of Liver Fibrosis Disease and Its Mathematical Results with Subinterval Transitions. *Fractal and Fractional* 8(11), (2024), 638.

[28] Shah, Kamal, Thabet Abdeljawad, and Arshad Ali. Mathematical analysis of the Cauchy type dynamical system under piecewise equations with Caputo fractional derivative. *Chaos, Solitons & Fractals* 161, (2022), 112356.

[29] Ali, Arshad, Kamal Shah, and Thabet Abdeljawad. Study of implicit delay fractional differential equations under anti-periodic boundary conditions. *Advances in Difference Equations* 2020(1), (2020), 139.

[30] Algolam, Mohamed S., Osman Osman, Arshad Ali, Alaa Mustafa, Khaled Aldwoah, and Amer Alsulami. Fixed Point and Stability Analysis of a Tripled System of Nonlinear Fractional Differential Equations with n-Nonlinear Terms. *Fractal & Fractional* 8(12), (2024), p697.

[31] Ali, Arshad, Khursheed J. Ansari, Hussam Alrabaiah, Ahmad Aloqaily, and Nabil Mlaiki. Coupled system of fractional impulsive problem involving power-law kernel with piecewise order. *Fractal and Fractional* 7(6), (2023), 436.

[32] F, Zhuo-Jia, et al. Numerical solutions of the coupled unsteady nonlinear convection-diffusion equations based on generalized finite difference method, *The European Physical Journal Plus* 134(6) (2019) 1-20.

[33] Naik, Parvaiz Ahmad, Mehmet Yavuz, Sania Qureshi, Jian Zu, and Stuart Townley. Modeling and analysis of COVID-19 epidemics with treatment in fractional derivatives using real data from Pakistan. *The European Physical Journal Plus* 135, (2020), 1-42.

[34] B. Wang, L. Li, Y. Wang, An efficient nonstandard finite difference scheme for chaotic fractional-order Chen system. *IEEE Access,* 8 (2020) 98410-98421.

[35] A.J.Arenas, G. González-Parra, B.M. Chen-Charpentier, Construction of nonstandard finite difference schemes for the SI and SIR epidemic models of fractional order, *Mathematics and Computers in Simulation,* 121 (2016) 48-63.

[36] D.Baleanu, S. Zibaei, M. Namjoo, A.Jajarmi, A nonstandard finite difference scheme for the modeling and nonidentical synchronization of a novel fractional chaotic system, *Advances in Difference Equations,* 2021(1) (2021)1-19.

Author information

Zia Ullah, Department of Natural Sciences and Humanities, University of Engineering and Technology Mardan 23200,, Pakistan.
E-mail: ziakhan9495@gmail.com

Muhammad Shoaib Arif, Department of Mathematics and Sciences, College of Humanities and Sciences, Prince Sultan University, Riyadh, 11586,, Saudi Arabia..
E-mail: marif@psu.edu.sa

Rahim Ud Din, Department of Mathematics, Air University, PAF Complex, Islamabad 44000,, Pakistan.
E-mail: rahimmaths24@gmail.com

Ikram Ullah, Department of Natural Sciences and Humanities, University of Engineering and Technology Mardan 23200,, Pakistan.
E-mail: ikram.ullah@uetmardan.edu.pk

Received: 2024-01-19
Accepted: 2025-05-14